

# Separating Inhibitory and Excitatory Responses of Epileptic Brain to Single-Pulse Electrical Stimulation

Sepehr Shirani

*Department of Computer Science, School of Science and Technology,  
Nottingham Trent University, United Kingdom  
E-mail: sepehr.shirani2021@my.ntu.ac.uk*

Antonio Valentin

*Department of Basic and Clinical Neuroscience, Institute of Psychiatry,  
Psychology and Neuroscience (IoPPN), King's College London, United Kingdom  
E-mail: antonio.valentin@kcl.ac.uk*

Gonzalo Alarcon

*The University of Manchester, United Kingdom  
E-mail: galarcon@aol.com*

Farhana Kazi

*Department of Basic and Clinical Neuroscience, Institute of Psychiatry,  
Psychology and Neuroscience (IoPPN), King's College London, United Kingdom  
E-mail: farhana.2.kazi@kcl.ac.uk*

Saeid Sanei\*

*Department of Computer Science, School of Science and Technology,  
Nottingham Trent University, United Kingdom  
E-mail: saeid.sanei@ntu.ac.uk*

To enable an accurate recognition of neuronal excitability in an epileptic brain for modelling or localization of epileptic zone, here the brain response to single-pulse electrical stimulation (SPES) has been decomposed into its constituent components using adaptive singular spectrum analysis (SSA). Given the response at neuronal level, these components are expected to be the inhibitory and excitatory components. The prime objective is to thoroughly investigate the nature of delayed responses (elicited between 100ms – 1s after SPES) for localization of the epileptic zone. SSA is a powerful subspace signal analysis method for separation of single channel signals into their constituent uncorrelated components. The consistency in the results for both early and delayed brain responses, verifies the usability of the approach.

*Keywords:* Delayed Response; Early Response; EEG; Epilepsy; Excitation; Inhibition; SPES; SSA.

## 1. Introduction

Epilepsy is one of the most common neurological disorders affecting at least 50 million people worldwide<sup>1</sup> and around 3.5 million people in Europe.<sup>2</sup> It is a chronic neurological disease characterized by epileptic events occurring due to excessive discharges of

neurons in the brain.<sup>3,4</sup> Due to the importance of epilepsy, the techniques for automatic detection of interictal epileptic form discharges (IEDs)<sup>5</sup> as well as seizure detection and prediction<sup>6,7</sup> have been investigated by a number of researchers. Moreover, in some recent studies, synchronization of brain corti-

cal signals has been used as an indicator of upcoming epileptic events.<sup>8</sup> As the Excitatory (E) and Inhibitory (I) activities are essential for regulating the flow of information in the brain, without evaluating and controlling the ratio between E and I activities, runaway excitation or inactivity would happen, hampering sufficient information processing.<sup>9–11</sup> A large number of previous studies have been focused on the role of excitation and inhibition in the transformation from normal condition to seizure in the epileptic brain.<sup>12</sup> The mechanisms underlying epileptic events previously have been thought to involve abnormal functioning of ion channels and synaptic activity leading to the E-I imbalance theory, (where increased E, decreased I, or both lead to a higher tendency for seizure generation and epileptogenesis). However, recent findings related to genetic mutation, the effect of neurotransmitters, the mechanism of anti-seizure medication, and metabolic factors in regulating neural excitability demand for reconsideration and expansion of the E-I imbalance hypothesis.<sup>13</sup> Since in partial epilepsy, an imbalance between E and I is expected in areas that induce epileptic events, in principle, cortical responses to electrical stimulation should help determine this imbalance.<sup>14</sup> A decent approach for studying the balance between E and I, applies single pulses, which activate only a limited and localized population of neurons. This technique, called single-pulse electrical stimulation (SPES), has been implemented for describing abnormal cortical responses to electrical pulses via intracranial electrodes.<sup>15–17</sup> According to previous research,<sup>17</sup> there are two types of responses to the SPES in the epileptic brain. First, early responses (ERs) are responses to SPES generally starting within the first 100ms after the stimulation artifact or sometimes merging with it. They consist of a sharp deflection often followed by a slow wave. While ERs are considered to be the brain’s normal reaction to the stimulation, the SPES method has established that regions showing the onset of spontaneous seizures are associated with distinct secondary responses to stimulation called delayed responses (DRs).<sup>17, 18</sup> DRs are responses starting with a delay longer than 100ms from the stimulation spike-shape artifact (generally between 100ms to 1s after stimulation). DRs often resemble spontaneous interictal discharges and are not seen after every stimulus. DRs have proved helpful in predicting seizure control after surgery, revealing the presence

of multiple epileptogenic areas, and identifying the epileptogenic cortical zone in patients with no seizure during data collection.<sup>14</sup> The results from previous research investigating the firing pattern alterations at the neural level in response to the SPES indicate that the firing patterns can be categorized into four groups where approximately 25% of neurons show a period of high-frequency burst, 14% show a period of suppression, 12% show high-frequency burst followed by suppression and approximately 50% show no change in the firing rate associated with the stimulation which further increases the stimulus location ranging from 49.7% for local stimulation to 81.6% for contralateral stimulation, suggesting that IED-like patterns can occur without involvement of all nearby neurons.<sup>19</sup> In our application, there is no access to the recordings of the firing pattern at the neural level from various regions for a large number of epileptic cases, including those who are the candidates for resection surgery. Therefore, here the aim is to decompose the SPES responses into orthogonal subspaces resulting in disjoint sources. The proposed approach was applied to the data recorded from the depth electrodes initially. However, due to the similarity of the responses to the SPES recorded from depth electrodes and ECoG, we also applied the method to ECoG.

Here, the single channel decomposition approach relies on the fact that the underlying signal components (i.e. E and I) originate from disjoint sources within the brain whereby can be separated. Due to the role of E-I imbalance in the epileptic brain, we aim to investigate the separability of E and I in both ERs and DRs using the data recorded from implanted electrodes. Furthermore, a separate investigation of E and I in response to SPES can offer great insight into a better understanding of the neural activity imbalance in regions associated with epileptic events in the brain.

## 2. Data Description

The intracranial electroencephalogram (EEG) was recorded at 256 Hz from 20 epileptic subjects at King’s College Hospital London as part of the clinical protocol for assessment of their conditions. The electrodes required to be implanted in the brain by surgical operation. Based on prior evaluation, the number, type, and locations of the intracranial electrodes were chosen by the suspected location of the

ictal onset region. The selection criteria and implantation procedure have been described previously<sup>20</sup> mainly for participants with drug resistant (refractory) epilepsy. The data from twenty patients have been recorded using the system and the method described by Kokkinos et al.<sup>21</sup> The SPES operation was carried out by applying the approved constant current of 1-8 mA, mostly 4 mA, from the neurostimulator through single pulse of 1 ms duration and 0.1 Hz frequency. Every 10 seconds a single monostatic pulse was applied while the EEG signals recorded from the electrodes not utilized for stimulation. Figure 1 illustrates an example of post-surgery computerized tomography (CT) scan showing the implanted subdural and depth electrodes in one subject. As demonstrated in Table 1, 11 out of 20 cases selected for this study underwent surgery after data acquisition, and the surgical operation outcomes are shown using Engel Outcome Scale.<sup>22</sup> Here, class-I refers to becoming (disabling) seizure free, class-II means rare disabling seizures, class-III indicates improvement in seizure reduction or prolonged seizure-free intervals, and class-IV means no worthwhile improvement. It is demonstrated in Table 1 that approximately 80% of the cases that underwent surgery experienced improvement, indicating the critical role of DRs in finding the location of epileptogenic neurons.

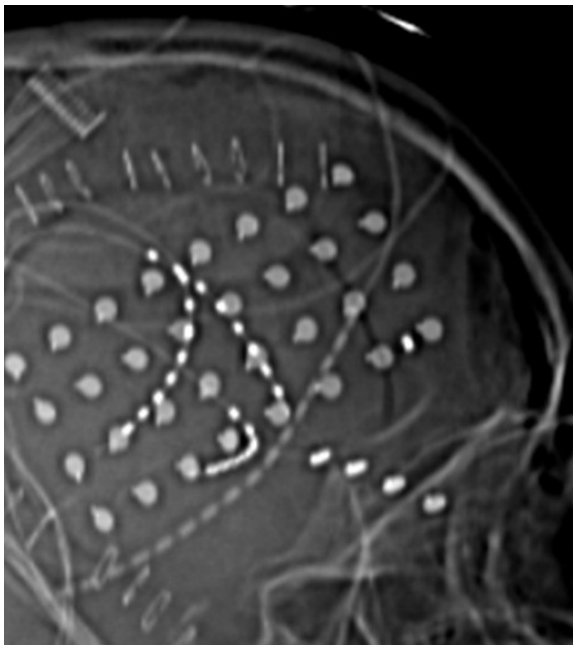


Figure 1. Post-surgery CT scan showing the implanted subdural and depth electrodes in one subject. (Elec-

trodes: 32 RT, 7 F, 7AT, 7 MidT, 4 PreF)

Table 1. The number and locations of the implanted electrodes alongside the result of the surgery for each case (R=Right, L=Left, T=Temporal, F=Frontal, A=Anterior, P=Posterior, O=Occipital, In=Insular, H=Hippocampus, Ms=Mesial, Par=Parietal).

case	Locations and number of implanted electrodes	Result of resection surgery (Engel Outcome Scale)
1	LT 40, LO 8, LMs 8, LF 8	No surgery
2	LTA 8, LTP 8, RT 8	I
3	LA 8, LPSubT 8, LF 8, LP 8	III
4	RF 8, RMidT 4, RPost 8, LA 8, LMidT 4, LP 8	IV
5	RT 40, RAT 8, RMsT 8, RPT 8	I
6	RF 8, RT 8, LF 8, LT 8	No surgery
7	SubF 8, F 8, TPole 8, AT 8, PT 16, TO 8, Par 8	No surgery
8	RAH 10, RMidH 10, RH 10, LAH 8, LMidH 10, LPH 10	I
9	RT 32, F 7, AT 7, MidT 7, PreF 4	No surgery
10	RT 32, Tpole 5, MidT 5, PMT 5, AIn 5, MidIn 5, PIn 5	II
11	RF 8, RSubT 8, LSubT 8	III
12	RT 32, AT 6, MidT 6	II
13	AF 8, PF 8, SupF 8, AT 8, MsT 8, PT 8	No surgery
14	RT 8, LT 8	No surgery
15	LT 20, F 8, IF 8, PF 8, ST 8	IV
16	RT 64, RTPole 5, RMsT 6	No surgery
17	Flns 4, TIns 4	No surgery
18	LT 64, LFP 8	I
19	RF 8, RT 8, LF 8, LT 8	No surgery
20	RMidF 10, RPF 10, LF 10	I

### 3. Method

In order to investigate the separability of E and I activities in ERs and DRs to the SPES, we apply a suitable subspace method to decompose these responses. Single-channel singular spectrum analysis (SSA) is a nonparametric method that can be applied to random statistical processes, whether linear or nonlinear, stationary or even mildly non-stationary, and Gaussian or non-Gaussian, without making prior assumptions about the data.<sup>23,24</sup> The main purpose of using SSA is its ability to separate the underlying components of single channel signals belonging to different subspaces. Due to this elegant property, it has found many applications in detection,<sup>25,26</sup> decomposition,<sup>27,28</sup> and forecasting.<sup>29,30</sup> According to the SSA properties and the fact that it performs well even for small sample sizes, it appears as a suitable method for investigating the ERs and DRs and separating each one into its I and E components. This is

mainly because these components fall into different orthogonal subspaces.

It is important to emphasize that the pipeline did not implement any frequency analysis approach for separation. Here, the intention is not to separate components with different asymmetries but inherently with different statistical distributions. SSA, regularized by statistical distributions, is used to decompose the data into orthogonal subspaces. However, after separating the components using SSA, we examined them in terms of their frequency ranges and it is clear that they fall perfectly in different frequency ranges.

Regarding the adopted pipeline in this research, it needs to be mentioned that the SSA method is not comparable with other decomposition methods, such as empirical mode decomposition (EMD) here, due to the purpose of this study. EMD decomposes the data into a number of intrinsic mode functions (IMFs) ordered in frequency. Conversely, SSA decomposes the data into its orthogonal components. Therefore, SSA is a better option where there is no clue in which domain the components are disjoint. SSA generally consists of two complementary stages. First, the signal is decomposed into its separate components, and in the second stage, the desired signals are reconstructed by grouping the orthogonal principal components. Here, a pipeline based on single-channel SSA has been followed in which, in the reconstruction stage, the eigentriples are adaptively selected. The above SSA stages together with the mathematical derivations have been described in the following sections.

### 3.1. Decomposition

The decomposition stage includes an embedding process followed by eigen decomposition. In the embedding process, after selecting a fixed window length of  $L$ , in the first step, the trajectory matrix  $\mathbf{X}$  that transfers the one-dimensional signal  $x$  of length  $T$  into the multi-dimensional series  $X_0, \dots, X_{K-1}$ , with vectors  $X_i = (x_i, \dots, x_{i+L-1})$  where  $K = T - L + 1$  is computed.

$$\mathbf{X} = (x_{i,j})_{i,j=0}^{L-1, K-1} = \begin{pmatrix} x_0 & x_1 & \cdots & x_{K-1} \\ \vdots & \ddots & & \vdots \\ x_{L-1} & x_L & \cdots & x_{T-1} \end{pmatrix}$$

In the next step  $\mathbf{S} = \mathbf{X}\mathbf{X}^T$  is factorized into its eigenvalues and eigenvectors to decompose trajectory ma-

trix  $\mathbf{X}$  into its orthogonal bases where in  $\mathbf{S} = \mathbf{U}\mathbf{\Lambda}\mathbf{U}^T$   $\mathbf{\Lambda}$  is the diagonal matrix of eigenvalues ordered so that  $\lambda_1 \geq \lambda_2 \geq \dots \lambda_L \geq 0$  and  $\mathbf{U} = (U_1, U_2, \dots, U_L)$  is the corresponding orthonormal matrix of eigenvectors of  $\mathbf{S}$ . Here,  $\mathbf{X} = X_1 + X_2 + \dots + X_d$ , where considering  $\mathbf{v}_i = X_i^T \mathbf{u}_i / \sqrt{\lambda_i}$  or  $X_i = \sqrt{\lambda_i} \mathbf{u}_i \mathbf{v}_i^T$ .

### 3.2. Reconstruction

The reconstruction stage corresponds to the selection of eigentriples into groups (eigentriple grouping) for the reconstruction of the one-dimensional time series by splitting the elementary matrices into several groups and summing the matrices in each group like  $\mathbf{X}_I = X_{I1} + X_{I2} + \dots + X_{Ip}$ . After grouping, diagonal averaging is used to transform the matrices into one-dimensional reconstructed signals like  $\tilde{x}_I$ . Here knowing that  $x_{ij} \in \mathbf{X}_I$ , the  $x_k \in \tilde{x}_I$  which is the  $k$ th term of the resulting time series  $\tilde{x}_I$  is  $Mean(x_{ij} | (i + j = k + 1))$ . In this study, for the reconstruction stage and regrouping the components, an adaptive approach has been developed and used after most of the noise-related eigentriples are removed. Following this method, the remaining components are grouped into two waveforms which best define the target E and I components. This is performed based on knowing that the E waveform has a spike shape with a peaky distribution implying high kurtosis. Therefore, during the grouping process the algorithm tends to separate a component with maximum kurtosis adaptively. To express the reconstruction of E component mathematically, we employ a diagonal matrix  $\mathbf{W}$  with binary diagonal elements, i.e.  $w_{jj} = \{0, 1\}$ . During the reconstruction process  $\mathbf{W}$  is iteratively estimated in order to achieve the maximum kurtosis, i.e.,

$$\mathbf{W}_{opt} = \max_{\mathbf{W}} (Kurt(\mathbf{W}\mathbf{\Lambda}^{\frac{1}{2}}\mathbf{V})) \quad (1)$$

where  $Kurt$  refers to Kurtosis. From Figure 2, the ER and DR waveforms are first decomposed into  $N$  separate components. Often (but not necessarily,) the first eigentriples represent the overall signal trend and the rest include low power activities such as noise, spikes, and low-amplitude oscillations. During the proposed adaptive process, and after discarding the very last (noise-related) components, the eigentriples related to the E waveform are grouped adaptively, (see Figure 2), to achieve the highest kurtosis. The result is expected to be the E waveform. This

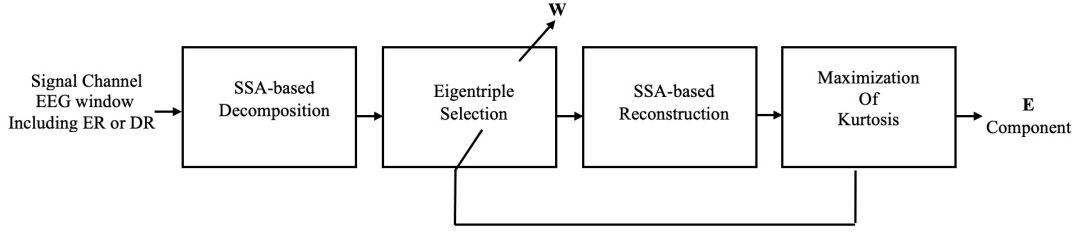


Figure 2. Block diagram of SSA system for E detection from ER or DR. The I component is obtained by subtraction of E and noise from the original EEG signal.

is then subtracted from the refined original signal to derive the I component. Looking at their temporal, power spectrum density (PSD), and time-frequency domain representations we can conclude that the components are disjoint and belong to orthogonal subspaces. This verifies that the E/I components naturally originate from independent sources and therefore are separable.

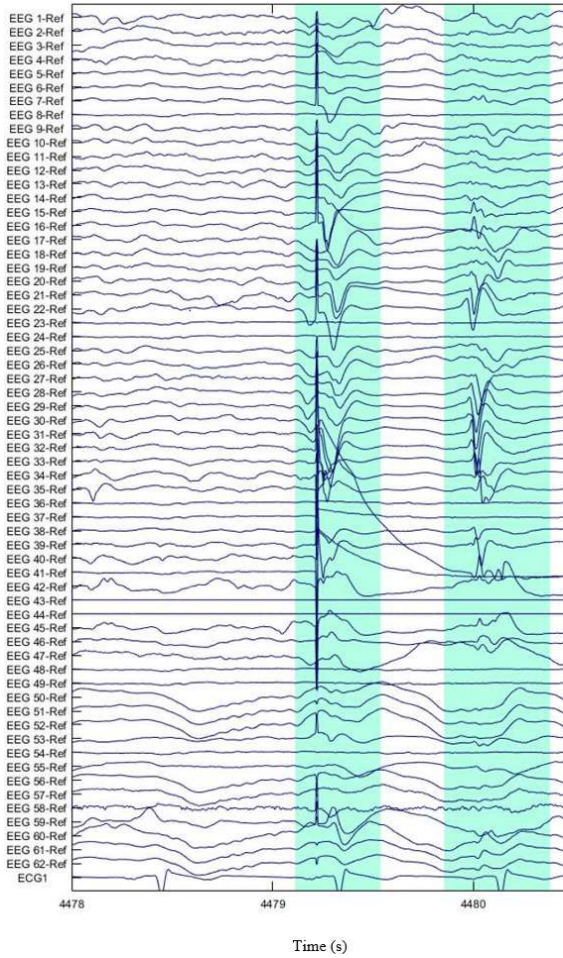


Figure 3. The ERs and DRs to the SPES visible in both

subdural and depth channels after SPES. The first 32 EEG channels are subdural, and the rest are depth electrodes. The last channel is ECG signal recorded from the subject.

#### 4. Results and Discussion

We used 300 selected segments from the 20 cases (subjects) included in this study, each 0.7 second long, containing the annotated ER or DR. Considering the length and shape of ERs and DRs in the data, a window length (aka embedding dimension) of 20 samples was selected for the SSA algorithm. After plotting the relative contribution and cumulative contribution to the trajectory (aka Hankel) matrix of components, the first  $N=10$  components were selected for regrouping. Figure 3 demonstrates an example of the ERs and DRs to the SPES in the intracranial EEG related to one of the subjects. After separating ERs and DRs, first, the E and I signals, and their power spectrum density were inspected. The results from ERs and DRs show that the I signal consists of EEG overall trend including the lower frequency oscillations with generally a narrow power spectrum density (PSD) concentrated in low frequencies up to approximately 10 Hz. However, the E signal consists of higher frequency oscillations with a lower power and wide PSD consisting of frequencies from between 10-20 Hz up to nearly 60 Hz. The frequency ranges for both I and E signals were slightly different for various subjects having different morphology responses. Figure 4 illustrates the results of the algorithm for an ER and DR recorded by a subdural electrode in the right temporal (RT) region and the PSD and the short-time Fourier transform (STFT) plot of E and I signals. As the images related to the ERs show, The electrical stimulation spike is considered as an artifact added to the ER obscuring the actual excitatory part of ER. This makes

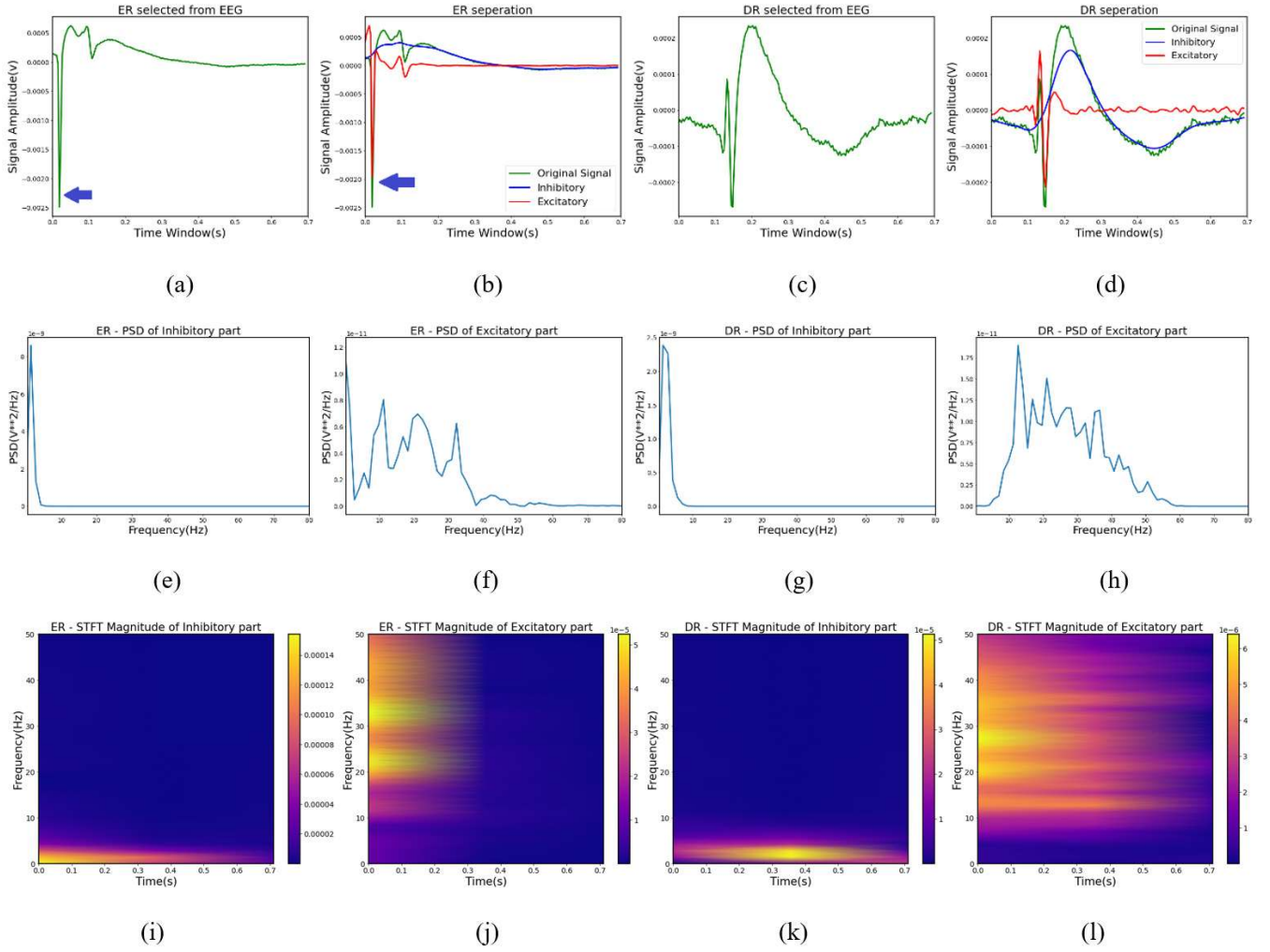


Figure 4. (a) An EEG segment including an ER elicited immediately after SPES (b) ER automatically decomposed into E and I parts (Here the arrow indicates the stimulus artifact mixed with the E part of response) (c) An EEG segment including a DR elicited with a delay after SPES (d) DR automatically decomposed into E and I parts (e) PSD of I activity for ER (f) PSD of E activity for ER (g) PSD of I activity for DR (h) PSD of E activity for DR (i) STFT magnitude of I activity for ER (j) STFT magnitude of E activity for ER (k) STFT magnitude of I activity for DR (l) STFT magnitude of E activity for DR. It is illustrated in the last row how effectively the two components have been separated using SSA.

evaluation of ER excitatory component difficult. To make sure that the noise removal process does not change the morphology of the SPES responses considerably, while sum of E and I remains similar to the selected overall SPES response, we use adaptive signed correlation index (ASCI).<sup>31</sup> The score is  $0.85 \pm 0.15$  for the tests that indicates the similarity of two waveforms. Also,  $C = (\sum_{j=0}^N E_j \times I_j) / L$  |  $j$ : samples has been measured to check the correlation between the E and I signals.  $C$  is close to zero for all the tests, illustrating that the E and I signals do not share the same subspaces. From the PSD and STFT magnitudes, the E and I signals can be in-

spected separately. The I-to-E power ratio is plotted for the selected ER and the related DR windows. The I-to-E power ratio plot demonstrates the changes for the selected windows. A consistent observation (approximately 75 percent of tests) is that in some channels where DRs are present after SPES, there is a considerable increase in the I-to-E power ratio after ERs and before DRs. Figure 5 illustrates the ratio for a selected window containing ER and the relative DR for a subdural channel implanted in the right temporal (RT) pole region.

As the I/E imbalance is considered a significant indicator of epilepsy in the epileptic brain and re-

gions associated with seizures,<sup>13</sup> investigating the E and I waveforms and the changes in the I/E ratio might help us to better understand the underlying information in DRs, and consequently, the overall seizure network in the future steps. The hypothesis is that, the epileptic zones contribute more to the elicitation of inhibition. Therefore, there can be more insight into seizure diagnosis and localization by deeper investigation of I-to-E power ratio for the DRs. One possible explanation for the severe and consistent increase in I-to-E power ratio before DRs in some channels might be their relative location and a short distance to the actual seizure onset zone or their association with regions in the seizure network. Previous studies have shown that DRs are generally observed in regions associated with seizure networks. Therefore, after stimulation of these regions, the role of DRs may be compensatory to prevent further increase of inhibition and synchronization between various regions, possibly leading to a seizure. Moreover, previous studies have shown the similarities between DRs and IEDs<sup>32</sup> and a possible explanation for the occurrence of IEDs to prevent seizures due to their high levels of inhibition indicated by the long suppression periods seen in single-cell activity.<sup>4</sup> Another possible explanation here is that the I-to-E ratio might affect the occurrence of DRs where the I-to-E ratio changes need to surpass a limit for elicitation of DRs even in regions capable of producing such responses to the SPES. Here, there is no statistically significant correlation between the location of the selected electrode and the observed alteration in the I-to-E ratio in the selected intervals. However, it is worth mentioning that most of the recording electrodes are implanted in the temporal area and naturally most of the DRs are observed in this region. Findings from a recent study highlight the important relationship between the morphology of the responses to the SPES and the location of the implanted electrodes. Based on this the local and distant cortical responses to SPES are differentially modulated by specific parameters like the intensity and location of the stimulation point in the brain.<sup>33</sup> Although the differences in the morphology of responses to the SPES (especially DRs), stemmed from different stimulation setup, makes it difficult to perform a direct comparison between these responses, the method proposed in this study offers the opportunity to investigate the E and I imbalance for the

recorded signals.

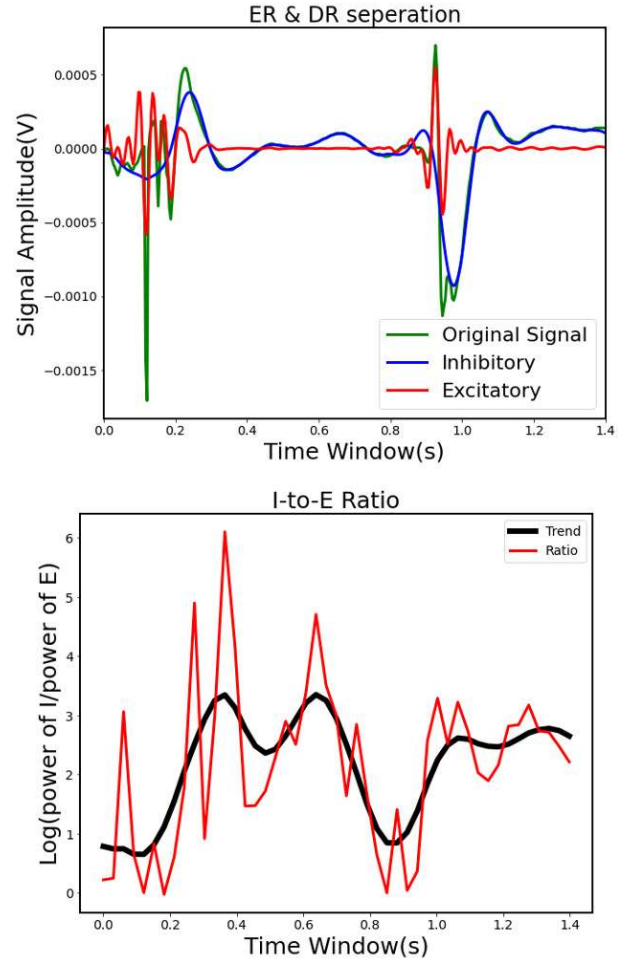


Figure 5. Logarithm of I-to-E power ratio for a selected EEG channel implanted in the right temporal (RT) pole region. (The bold black curve shows the smoothed trend)

To better discover if the I-to-E ratio measurements explicitly estimated based on our proposed method can be used to explain the DRs some points need to be considered. First, the proposed approach was initially applied to the data recorded from the depth electrodes. However, due to the similarity of the responses to the SPES recorded from depth electrodes and ECoG, we also applied the method to ECoG signals. The depth electrodes permit recording the activity from a local and specific region from a much smaller group of neurons, whereas ECoG records a superposition of activities from different sources in the brain. Therefore, the decomposed components from ECoG signals are more likely the result of synchronized activities for a population of neu-

rons. The E activity is more localized than the I activity; therefore, it can affect the observed separated components and I-to-E power ratio in subdural (ECoG) electrodes compared to depth electrodes. Second, the DRs, seen in multiple depth electrodes, sometimes demonstrate different behavior in terms of E and I activities and the ratio between them and they have differences in their morphologies. It is possible that the DRs or part of them in some depth channels are actually from a propagated signal from a nearby source. Finally, it needs to be mentioned that the SSA algorithm performance in terms of separating the input into distinguishable components differs according to the morphology of the signal. Therefore, an adaptive approach for selecting SSA parameters like signal and window length is worth being investigated.

## 5. Conclusion

In this study, for the first time, we presented an approach based on SSA with an adaptive reconstruction step to investigate the separability of E and I activities for both ERs and DRs to the SPES for the epileptic brain, where an imbalance between E and I is expected. The majority of EEG-based studies refer to E and I activities based on the frequency of the waveforms without referring to their frequency ranges. However, the method used here exploits the waveform morphology, and that the components are disjoint using subspace decomposition. This paves the path for deeper investigation of seizure network, excitability of the brain tissue, localization of epileptic neurons, and extracting other possible information which can be used for seizure treatment particularly by using deep brain stimulation.

## References

1. C. Behr, M. Goltzene, G. Kosmalski, E. Hirsch, and P. Ryvlin, "Epidemiology of epilepsy," *Revue Neurologique*, vol. 172, no. 1, pp. 27–36, 2016.
2. L. Forsgren, E. Beghi, A. Oun, and M. Sillanpää, "The epidemiology of epilepsy in europe—a systematic review," *European Journal of Neurology*, vol. 12, no. 4, pp. 245–253, 2005.
3. U. R. Acharya, S. V. Sree, G. Swapna, R. J. Martis, and J. S. Suri, "Automated EEG analysis of epilepsy: a review," *Knowledge-Based Systems*, vol. 45, pp. 147–165, 2013.
4. G. Alarcón, J. Martínez, S. V. Kerai, M. E. Lacruz, R. Q. Quiroga, R. P. Selway, M. P. Richardson, J. J. G. Seoane, and A. Valentín, "In vivo neuronal firing patterns during human epileptiform discharges replicated by electrical stimulation," *Clinical Neurophysiology*, vol. 123, no. 9, pp. 1736–1744, 2012.
5. B. Abdi-Sargezeh, A. Valentin, G. Alarcon, and S. Sanei, "Incorporating uncertainty in data labeling into automatic detection of interictal epileptiform discharges from concurrent scalp-EEG via multi-way analysis," *International Journal of Neural Systems*, vol. 31, no. 08, p. 2150019, 2021.
6. H. S. Nogay and H. Adeli, "Detection of epileptic seizure using pretrained deep convolutional neural network and transfer learning," *European Neurology*, vol. 83, no. 6, pp. 602–614, 2020.
7. A. Bhattacharya, T. Baweja, and S. Karri, "Epileptic seizure prediction using deep transformer model," *International Journal of Neural Systems*, vol. 32, no. 02, p. 2150058, 2022.
8. A. Olamat, P. Ozel, and A. Akan, "Synchronization analysis in epileptic EEG signals via state transfer networks based on visibility graph technique," *International Journal of Neural Systems*, vol. 32, no. 02, p. 2150041, 2022.
9. H. Bruining, R. Hardstone, Juarez-Martinez *et al.*, "Measurement of excitation-inhibition ratio in autism spectrum disorder using critical brain dynamics," *Scientific Reports*, vol. 10, no. 1, pp. 1–15, 2020.
10. O. Kinouchi and M. Copelli, "Optimal dynamical range of excitable networks at criticality," *Nature Physics*, vol. 2, no. 5, pp. 348–351, 2006.
11. G. G. Turrigiano and S. B. Nelson, "Homeostatic plasticity in the developing nervous system," *Nature Reviews Neuroscience*, vol. 5, no. 2, pp. 97–107, 2004.
12. K. Staley, "Molecular mechanisms of epilepsy," *Nature Neuroscience*, vol. 18, no. 3, pp. 367–372, 2015.
13. L.-R. Shao, C. W. Habela, and C. E. Stafstrom, "Pediatric epilepsy mechanisms: expanding the paradigm of excitation/inhibition imbalance," *Children*, vol. 6, no. 2, p. 23, 2019.
14. A. Valentín, G. Alarcón, M. Honavar, J. J. G. Seoane, R. P. Selway, C. E. Polkey, and C. D. Binnie, "Single pulse electrical stimulation for identification of structural abnormalities and prediction of seizure outcome after epilepsy surgery: a prospective study," *The Lancet Neurology*, vol. 4, no. 11, pp. 718–726, 2005.
15. G. Alarcón, D. Jiménez-Jiménez, A. Valentín, and D. Martín-López, "Characterizing EEG cortical dynamics and connectivity with responses to single pulse electrical stimulation (SPES)," *International Journal of Neural Systems*, vol. 28, no. 06, p. 1750057, 2018.
16. D. Flanagan, A. Valentín, J. J. García Seoane, G. Alarcón, and S. G. Boyd, "Single-pulse electrical stimulation helps to identify epileptogenic cortex



- in children,” *Epilepsia*, vol. 50, no. 7, pp. 1793–1803, 2009.
17. A. Valentin, M. Anderson, G. Alarcon, J. G. Seoane, R. Selway, C. Binnie, and C. Polkey, “Responses to single pulse electrical stimulation identify epileptogenesis in the human brain in vivo,” *Brain*, vol. 125, no. 8, pp. 1709–1718, 2002.
  18. A. Valentin, G. Alarcon, J. J. Garcia-Seoane, M. Lacruz, S. Nayak, M. Honavar, R. P. Selway, C. Binnie, and C. Polkey, “Single-pulse electrical stimulation identifies epileptogenic frontal cortex in the human brain,” *Neurology*, vol. 65, no. 3, pp. 426–435, 2005.
  19. G. Alarcón, J. Martínez, S. V. Kerai, M. E. Lacruz, R. Q. Quiroga, R. P. Selway, M. P. Richardson, J. J. G. Seoane, and A. Valentín, “In vivo neuronal firing patterns during human epileptiform discharges replicated by electrical stimulation,” *Clinical Neurophysiology*, vol. 123, no. 9, pp. 1736–1744, 2012.
  20. J. Engel, *Surgical treatment of the epilepsies*. Raven Press, 1987.
  21. V. Kokkinos, G. Alarcón, R. P. Selway, and A. Valentín, “Role of single pulse electrical stimulation (SPES) to guide electrode implantation under general anaesthesia in presurgical assessment of epilepsy,” *Seizure*, vol. 22, no. 3, pp. 198–204, 2013.
  22. J. Engel, “Update on surgical treatment of the epilepsies: summary of the second international palm desert conference on the surgical treatment of the epilepsies (1992),” *Neurology*, vol. 43, no. 8, pp. 1612–1612, 1993.
  23. J. B. Elsner and A. A. Tsonis, *Singular spectrum analysis: a new tool in time series analysis*. Springer Science and Business Media, 1996.
  24. S. Sanei and H. Hassani, *Singular Spectrum Analysis of Biomedical Signals*. CRC press, 2015.
  25. S. Sanei, T. K. Lee, and V. Abolghasemi, “A new adaptive line enhancer based on singular spectrum analysis,” *IEEE Transactions on Biomedical Engineering*, vol. 59, no. 2, pp. 428–434, 2011.
  26. F. Ghaderi, H. R. Mohseni, and S. Sanei, “Localizing heart sounds in respiratory signals using singular spectrum analysis,” *IEEE Transactions on Biomedical Engineering*, vol. 58, no. 12, pp. 3360–3367, 2011.
  27. S. Kouchaki, S. Sanei, E. L. Arbon, and D.-J. Dijk, “Tensor based singular spectrum analysis for automatic scoring of sleep EEG,” *IEEE Transactions on Neural Systems and Rehabilitation Engineering*, vol. 23, no. 1, pp. 1–9, 2014.
  28. S. Sanei, M. Ghodsi, and H. Hassani, “An adaptive singular spectrum analysis approach to murmur detection from heart sounds,” *Medical Engineering and Physics*, vol. 33, no. 3, pp. 362–367, 2011.
  29. M. Ghil and N. Jiang, “Recent forecast skill for the el nino/southern oscillation,” *Geophysical Research Letters*, vol. 25, no. 2, pp. 171–174, 1998.
  30. K. Patterson, H. Hassani, S. Heravi, and A. Zhigljavsky, “Multivariate singular spectrum analysis for forecasting revisions to real-time data,” *Journal of Applied Statistics*, vol. 38, no. 10, pp. 2183–2211, 2011.
  31. A. Olenko, K. T. Wong, H. Mir, and H. Al-Nashash, “Generalised correlation index for quantifying signal morphological similarity,” *Electronics Letters*, vol. 52, no. 22, pp. 1832–1834, 2016.
  32. D. Nayak, A. Valentín, R. P. Selway, and G. Alarcón, “Can single pulse electrical stimulation provoke responses similar to spontaneous interictal epileptiform discharges?” *Clinical Neurophysiology*, vol. 125, no. 7, pp. 1306–1311, 2014.
  33. A. C. Paulk, R. Zemann, B. Crocker *et al.*, “Local and distant cortical responses to single pulse intracranial stimulation in the human brain are differentially modulated by specific stimulation parameters,” *Brain Stimulation*, vol. 15, no. 2, pp. 491–508, 2022.